

1 **Histone deacetylase 9 promoter hypomethylation associated with adipo-**
2 **cyte dysfunction is a statin-related metabolic effect**

3

4 Amna Khamis^{1,2}, Raphael Boutry², Mickaël Canouil², Sumi Mathew¹, Stephane Lob-
5 bens², Hutokshi Crouch¹, Toby Andrew¹, Amar Abderrahmani², Filippo Tamanini¹,
6 Philippe Froguel^{1,2*}.

7

8 ¹Department of Metabolism, Section of Genomics and Genetics, Imperial College
9 London, UK

10 ²Univ. Lille, CNRS, Institut Pasteur de Lille, UMR 8199 - EGID, F-59000 Lille, France

11

12 *Corresponding author

13

14

15

16

17

18

19

20

21

22

23

24

25

26 **Abstract**

27 **Background**

28 Adipogenesis, the process whereby preadipocytes differentiate into mature adipo-
29 cytes, is crucial for maintaining metabolic homeostasis. Cholesterol lowering statins
30 increase type 2 diabetes (T2D) risk possibly by affecting adipogenesis and insulin
31 resistance but the (epi)genetic mechanisms involved are unknown. Here, we charac-
32 terised the effects of statin treatment on adipocyte differentiation using *in vitro* human
33 preadipocytes cell model to identify putative effective genes.

34 **Results**

35 Statin treatment during adipocyte differentiation caused a reduction in key genes in-
36 volved in adipogenesis, such as *ADIPOQ*, *GLUT4* and *ABCG1*. Using Illumina's Infin-
37 ium '850K' Methylation EPIC array, we found a significant hypomethylation of
38 cg14566882, located in the promoter of the histone deacetylase 9 (*HDAC9*) gene, in
39 response to two types of statins (atorvastatin and mevastatin), which correlates with
40 an increased *HDAC9* mRNA expression. *HDAC9* is a transcriptional repressor of the
41 cholesterol efflux *ABCG1* gene expression, which is epigenetically modified in obesity
42 and prediabetic states. Thus, we assessed the putative impact of *ABCG1* knockdown
43 in mimicking the effect of statin in adipogenesis. *ABCG1* KD reduced the expression
44 of key genes involved in adipocyte differentiation and decreased insulin signalling
45 and glucose uptake. In human blood cells from two cohorts, *ABCG1* expression was
46 impaired in response to statins, confirming that *ABCG1* is *in vivo* targeted by these
47 drugs.

48 **Conclusions**

49 We identified an epigenetic link between adipogenesis and adipose tissue insulin re-
50 sistance in the context of T2D risk associated with statin use, which has important

51 implications as HDAC9 and ABCG1 are considered potential therapeutic targets for
52 obesity and metabolic diseases.

53 **Keywords**

54 Adipogenesis, methylation, ABCG1, HDAC9

55 **1 Background**

56 Adipose tissue plays a crucial role in regulating insulin sensitivity and glucose ho-
57 meostasis (1). In obesity, adipose expansion occurs as a result of cellular hypertro-
58 phy, *i.e.*, the increase in size of the adipocyte, and/or *de novo* adipogenesis, which is
59 the production of new mature adipocytes from residing preadipocytes (2–4). Dysregu-
60 lation in the adipogenic process is associated with metabolic diseases and insulin
61 resistance (5) and is an independent risk factor for type 2 diabetes (T2D) (6). In con-
62 trast, appropriate adipocyte expansion is protective against T2D in the context of
63 obesity (7,8). Adipogenesis occurs as a result of metabolic cues that trigger the in-
64 duction of key differentiation regulators, such as ADIPOQ, FASN, PPAR γ , ABCG1
65 and GLUT4 (9–12). Epigenome wide association studies (EWAS) have found that
66 hypermethylation within one of these genes involved in adipogenesis, *ABCG1*, was
67 associated with increased body mass index (BMI), insulin resistance and T2D risk
68 (13–16), opening avenues in the elucidation of the links between adipogenesis and
69 metabolic diseases.

70 One of the most common drugs known to modulate adipogenesis are statins (17).

71 The clinical use of statin is associated with an increased risk of insulin resistance and
72 T2D risk (18), but the molecular mechanisms involved remain poorly understood. We
73 hypothesised that statin treatment modulates adipogenesis by modifying the adipo-
74 cyte epigenome. In this study, we confirmed the inhibitory effects of statin treatment

75 in human preadipocytes and investigated the whole methylome to identify potential
76 regulators that may be involved in adipogenesis.

77 **2 Results**

78 2.1 Statin treatment reduced adipogenesis and insulin signalling

79 The Simpson-Golabi-Behmel syndrome (SGBS) human preadipocyte cell line was
80 used in this study as an *in vitro* model for adipocyte differentiation. In SGBS cells,
81 lipid droplet formation occurred by 12-14 days of differentiation together with an in-
82 crease in the expression of key adipogenic markers (19). We retrieved adequate
83 SGBS cell morphology modification and formation of lipids droplets by day 12 (Addi-
84 tional File 1: Figure S1a), and observed that the expression of key genes involved in
85 adipocyte differentiation and maturation was accordingly up-regulated (Additional File
86 1: Figure S1b).

87 For statin treatment, SGBS cells were differentiated for 6 days and then treated with
88 atorvastatin and mevastatin for an additional 6 days until final maturation (Figure 1a).
89 We observed a clear decrease in lipid-droplet formation in statin-treated SGBS cells
90 (both atorvastatin and mevastatin) when compared to DMSO-vehicle controls (Figure
91 1b). We also found that statin-treatment induced a significant down-regulation of
92 many key genes associated with adipogenesis reported above (*ABCG1*, *LEPTIN* and
93 *GLUT4*), with the particular exclusion of *PPARG*, a gene known to play a role only in
94 the early stages of adipocytes differentiation (Figure 1c). We then measured the ef-
95 fects of statin on downstream regulators of insulin signalling and found decreased
96 efficiency of insulin to activate ERK and AKT (Figure. 1d). Taken together, the data
97 support the inhibitory effects of statin in the human adipocyte differentiation and insu-
98 lin signalling, a similar effect reported in statin-treated 3T3-L1 mouse adipocyte cells
99 (17).

100

101 2.2 Whole methylome analysis of statin-treated SGBS cell line

102 To identify potential regulators involved in statin-induced adipocyte dysregulation, we
103 performed an unbiased whole methylation analysis in statin-treated SGBS cells using
104 Illumina's Infinium '850K' Methylation EPIC arrays (Additional File 1: Figure S2). We
105 filtered differentially methylated positions (DMPs) located in the promoter region, an-
106 notated as TSS200 or TSS1500 (within 200-1500 base pairs from the transcription
107 start site), in order to identify DMPs that were likely to have a biological effect. The
108 most significant DMP was cg14566882, located in the promoter of the histone deace-
109 tylase (*HDAC9*) gene, in mevastatin-treated cells ($\beta = 8.28\%$; $p = 5.55 \times 10^{-6}$) (Figure
110 2a). This DMP was also significantly hypomethylated in response to atorvastatin
111 treatment, compared to DMSO-vehicle controls ($\beta = 5.53\%$; $p = 1.35 \times 10^{-3}$) (Figure
112 2a, b).

113 Additionally, 87 DMPs were shared between the mevastatin and atorvastatin-treated
114 groups (Additional File 2: Table 1) and of the hypomethylated DMPs, cg14566882 in
115 *HDAC9* remained the top candidate in both atorvastatin and mevastatin treatments
116 (Additional File 1: Figure S3). A significant differentially methylated region (DMR)
117 overlapping this promoter region was also found in response to both treatments (Ad-
118 ditional File 1: Figure S4; False discovery rate < 0.05). In order to validate the effect
119 of cg14566882 hypomethylation on the expression of the *HDAC9* gene, we per-
120 formed qPCRs in statin-treated SGBS cell lines and found significant up-regulation of
121 the *HDAC9* gene at the mRNA level ($p < 0.05$; atorvastatin: 14-fold; mevastatin: 11-
122 fold) (Figure 2c).

123 ABCG1 has been reported to be regulated by HDAC9-mediated changes in acetyla-
124 tion (20,21) and may be targeted by the *HDAC9* epigenetic alteration. We confirmed

125 that ABCG1 protein expression is indeed down-regulated in response to mevastatin
126 and atorvastatin treatment (Figure 2d). We confirmed that in response to statin, this
127 effect was independent of the previously reported hypermethylation in cg06500161
128 (p-value > 0.5) and cg27243685 (p-value > 0.5) found to be associated with in-
129 creased BMI and T2D incidence (Additional File 1: Table 2) (15,22–24).

130

131 2.3 Knockdown of *ABCG1* in SGBS preadipocytes reduced adipocyte differentiation

132 We performed an *ABCG1* knockdown (KD) in SGBS cells to address whether re-
133 duced *ABCG1* expression mimics the effect of statins in adipogenesis. SGBS preadi-
134 pocytes were stably transfected with a shRNA targeting *ABCG1* mRNA and followed
135 them quantitatively through maturation and differentiation and this data was com-
136 pared with cells transfected with a non-targeting shRNA (control). A similar protocol
137 for stably knockdown *Abcg1* via shRNA has previously been achieved and described
138 in mouse 3T3-L1 preadipocytes (25). We initially analysed the expression of ABCG1
139 protein in normal adipocytes to show that it is positively associated with adipogenesis
140 as ABCG1 starts to become expressed at day 6 of differentiation (Figure 3a). The
141 efficient silencing of *ABCG1* (*ABCG1* KD) was confirmed at the protein level (Figure
142 3b). *ABCG1* KD in SGBS cells was accompanied by a significant reduction in the lipid
143 content (20 % reduction, $p < 0.05$; Figure 3c), along with the down-regulation of the
144 following adipocyte differentiation markers *FASN*, *PPARG* and *PLIN1* and key adipo-
145 cyte maturation markers *ADIPOQ* and *GLUT4* (Figure 3d). As a consequence of im-
146 paired adipogenesis, the *ABCG1* KD led to a significant reduction in glucose uptake
147 stimulated by insulin (65 % reduction, $p < 0.001$; Figure 3e). In addition, we found a
148 decreased efficiency of insulin to activate AKT in those cells (Figure 3f). As a whole,

149 this data indicates that *ABCG1* levels are pivotal for the control of human adipocyte
150 differentiation and glucose metabolism.

151 2.4 *ABCG1* is down-regulated in response to statin in human blood samples

152 We next explored whether *ABCG1* was also dysregulated in samples from human
153 subjects. We analyzed reported transcriptomic data from blood samples from two
154 cohorts. The first consisted of a total of 57 individuals from the ECLIPSE cohort, of
155 which 13 were statin users (26). A significant reduction in the expression of *ABCG1*
156 in the statin group ($p = 1.41 \times 10^{-5}$) was found, compared to non-users (Figure 4a). In
157 addition, we also analysed data from the YELLOW II study (27), a retrospective study
158 following 85 individuals before and following an extensive 8-12 week statin therapy.
159 In peripheral blood mononuclear cells obtained from blood samples, *ABCG1* expres-
160 sion was significantly decreased following statin treatment, compared to baseline
161 levels, for two *ABCG1* probes (ILMN_1794782 $p = 2.76 \times 10^{-5}$; ILMN_2329927 $p =$
162 4.28×10^{-4}) (Figure 4b). Taken together, this demonstrates that *ABCG1* reduction in
163 response to statin is indeed reflected in human blood samples. Of note, no data on
164 *HDAC9* expression was available in the ECLIPSE case control study, and no signifi-
165 cant change in *HDAC9* expression was reported in the intervention YELLOW II study,
166 maybe due to the lack of sufficient statistical power of this study.

167

168 **3 Discussion**

169 A recent 15 year prospective study found a staggering 38 % increased incidence of
170 T2D in statin users, regardless of the type of statin used (28). Here, we report that
171 two statins, atorvastatin and mevastatin, hamper the differentiation process in the
172 SGBS human preadipocyte cell line and decreased insulin sensitivity.

173 We focused our analysis on promoter DMPs, which are normally inversely correlated
174 with expression (29,30). Therefore, not surprisingly, given the inhibitory effect of
175 statin, our whole methylome analysis revealed that most DMPs were hypermethy-
176 lated. This includes the *IDI1* gene, which encodes the isopentenyl diphosphate isom-
177 erase, a component of the cholesterol synthesising pathway (31,32).

178 We report for the first time that statin treatment was associated with a significant hy-
179 pomethylation of *HDAC9* promoter, which is inversely correlated with *HDAC9* gene
180 expression. These findings are of particular significance in light of several studies that
181 demonstrated the key role of HDAC9 in adipocytes function: overexpression of
182 *Hdac9* in 3T3-L1 preadipocyte mouse cell lines suppressed adipogenesis and in-
183 versely, preadipocytes isolated from *Hdac9* knockout mice had an accelerated adipo-
184 cyte differentiation (33). Furthermore, *Hdac9* knockout mice showed improved meta-
185 bolic homeostasis and were protected from adipose tissue dysfunction in mice fed on
186 a high fat feeding (34). These studies clearly indicate the deleterious role of HDAC9
187 in maintaining adipocytes homeostasis both *in vitro* and *in vivo*.

188 *HDAC9*-deficient macrophages and monocytes directly increased the accumulation
189 of total acetylated H3 and H3K9 at the promoter of the *ABCG1* gene (20,21), thereby
190 inducing the transcription of the *ABCG1* gene, indicating that HDAC9 mediates the
191 expression of *ABCG1* through promoter-mediated acetylation. This is of particular
192 interest, as several studies have reported a role of ABCG1 in obesity, insulin resis-
193 tance and T2D. Elevated *ABCG1* expression is associated with increased fat mass
194 from obese individuals, suggesting that *ABCG1* is also involved in human adipo-
195 genesis (25). Although genome-wide association studies have not found any single
196 nucleotide polymorphisms (SNPs) within or nearby *ABCG1* associated with increased
197 T2D risk, several EWAS have found that hypermethylation in the *ABCG1* gene was

198 associated with fasting glucose, HbA1C levels, lipid metabolism, fasting insulin, T2D
199 risk and BMI (15,16,22,35–38). Additional observations in mouse models have shown
200 that *Abcg1*^{-/-} mice were protected from high fat diet-induced glucose intolerance (39).
201 A recent study found that *ABCG1* expression is reduced in both subcutaneous and
202 visceral adipose tissue in morbidly obese patients with metabolic syndrome com-
203 pared to those without metabolic syndrome, providing further evidence for a role of
204 *ABCG1* in the maintenance of metabolic homeostasis in adipocytes (40). In addition,
205 two studies showed that *ABCG1* expression was decreased in blood white human
206 cells in response to statins. As *ABCG1* was down-regulated in response to statin, we
207 hypothesised that *ABCG1* plays a role in statin-induced adipocyte dysregulation.
208 Indeed, we showed that *ABCG1* expression increases during human SGBS adipo-
209 cyte differentiation and through *ABCG1* silencing, confirm that the level of *ABCG1*
210 expression is crucial for the appropriate expression of lipid metabolism markers,
211 which include *FASN*, *FABP4*, *PLIN1* and *PPARG*, for correct human adipocyte differ-
212 entiation. Our findings are consistent with previous data showing variation in these
213 four genes following *Abcg1* silencing in mouse 3T3-L1 pre-adipocyte cells (41). The
214 down-regulation of *GLUT4* in *ABCG1* KD suggested a decrease in insulin-induced
215 glucose uptake. Indeed, we confirmed a down-regulation of phosphorylation of AKT
216 and ERK. Collectively this data indicates that normal *ABCG1* function is required for
217 adipogenesis and insulin signalling. In addition, we have confirmed using two sepa-
218 rate datasets that statin use was indeed correlated with a reduction in *ABCG1* ex-
219 pression in human blood samples. Other studies have reported a link between
220 *ABCG1* downregulation and diabetes incidence (42) and high fasting glycaemia (43).
221 Taken together, our human cellular data is consistent with human observational stud-

222 ies, in which the inhibition of *ABCG1* expression was deleterious for metabolism in
223 adipose tissue.

224 **Conclusions**

225 The model proposed based on our data from statin-induced insulin resistance is hy-
226 pomethylation of the *HDAC9* promoter induces *HDAC9* gene expression, which in
227 turn blocks *ABCG1* expression and thereby adipocyte differentiation and metabolic
228 dysfunction (Figure 5). Adipocyte turnover by adipogenesis is crucial for the mainte-
229 nance of metabolic homeostasis and insulin sensitivity (44). Our data provides a
230 novel epigenetic link between adipogenesis dysfunction and insulin resistance, medi-
231 ated by statins. The increased understanding of adipogenesis provides a promising
232 new avenue for the treatment of metabolic disease in obesity (9,44). Both HDAC9 and
233 ABCG1 have been proposed as therapeutic targets for patients with obesity in sepa-
234 rate previous studies (34,41), however, our data support a mechanistic pathway link-
235 ing them to metabolic diseases.

236 **4 Methods**

237 4.1 Cell culture and differentiation of SGBS cell line

238 SGBS human preadipocyte cell line was kindly provided by Prof. Dr. M. Wabitsch
239 (University of Ulm, Germany) and maintained in DMEM/F12 supplemented with 10 %
240 foetal bovine serum and 0.01 % penicillin/streptomycin (15140-122 - Life Technolo-
241 gies), as previously described (19). Confluent preadipocytes were differentiated un-
242 der serum-free culture conditions by washing twice with phosphate buffered saline
243 (PBS) and then exposing to DMEM/F12 supplemented with 2 $\mu\text{mol/l}$ rosiglitazone, 25
244 nmol/l dexamethasone, 0.5 mmol/l methylisobutylxantine, 0.1 $\mu\text{mol/l}$ cortisol, 0.01
245 mg/ml transferrin, 0.2 nmol/l triiodothyronin, and 20 nmol/l human insulin for 4 days.
246 The cells were then cultured for a further 8 days in fresh DMEM/F12 supplemented

247 with 0.1 $\mu\text{mol/l}$ cortisol, 0.01 mg/ml transferrin, 0.2 nmol/l triiodotyronin, and 20 nmol/l
248 human insulin. Microscopic images of SGBS cells were taken under a microscope
249 (IT404; VWR) using the Motic Image plus version 2.0 (Motic Europe).

250

251 4.2 Treatment with statins

252 At 6 days of differentiation, SGBS cells were treated with 10 μM mevastatin (M2537,
253 Sigma Aldrich) or atorvastatin (PZ0001, Sigma Alrich) and compared to a Dimethyl
254 sulfoxide (DMSO)-vehicle control (D2650, Sigma Aldrich). The cells were then incu-
255 bated for a further 6 days. On day 12 of differentiation, cells collected for further
256 analysis.

257 4.3 Whole methylome analysis

258 DNA was extracted from SGBS cells treated with atorvastatin and mevastatin at day
259 6 for 6 days and collected the cells at day 12. DNA was extracted using the Nucleo-
260 Spin Tissue kit (Takara Bio). Bisulfite conversion of 500 ng genomic DNA was per-
261 formed using the EZ-96 DNA Methylation kit (Zymo Research) following the manufac-
262 turer's protocol. Bisulfite-converted DNA was subjected to genome-wide DNA methy-
263 lation analysis using Illumina's Infinium '850K' Methylation EPIC array to identify dif-
264 ferentially methylated positions (DMPs). The resulting DNA methylation IDAT files
265 were imported using the *minfi* R package for further processing and quality control
266 (45). The following CpG probes were excluded from further analysis: probes on sex
267 chromosomes, cross-hybridising probes, non-cg probes and probes that lie near sin-
268 gle nucleotide polymorphisms (SNPs). Probe-design biases and batch effects were
269 normalised using R packages *ENmix* (46) and *SVA* (ComBat) (47), respectively.
270 To identify DMPs, the R package *limma* was used (48). The model included treat-
271 ment (atorvastatin, mevastatin or DMSO-vehicle) as a categorical variable and repli-

272 cates / day of experiment as a covariate. Methylation levels denoted by beta-values,
273 where 0 indicates 0 % methylation and 1 indicates 100 % methylation, were trans-
274 formed to M-values (49). To identify differentially methylated regions (DMRs), the R
275 package *DMRcate* was used (50). *DMRcate* ranks the differentially methylated re-
276 gions across the genome using Gaussian kernel smoothing based on the DMPs.

277 4.4 RNA extraction, cDNA conversion and RT-PCR

278 Total RNA was extracted from cultured cells using a RiboPure RNA Purification Kit
279 (AM1924; Invitrogen), according to the manufacturer's instructions and quantified on
280 a NanoDrop Spectrophotometer (Thermo Scientific). RNA was reverse transcribed
281 using a High-Capacity RNA-to-cDNA Kit (4387406; Applied Biosystems), according
282 to the manufacturer's instructions. qPCRs were conducted on an Applied Biosystems
283 7900HT Fast Real-Time PCR System and quantitative expression levels were ob-
284 tained using the SDS v2.3 Software (Applied Biosystems) using Taqman Gene Ex-
285 pression Assays (ThermoFisher Scientific). The following probes were used: *ABCG1*
286 (Hs01555193_m1), *CEBPB* (Hs00270923_s1), *LPL* (Hs00173425_m1), *ACACA*
287 (Hs01046047_m1) *FABP4* (Hs01086177_m1), *GLUT4* (Hs00168966_m1), *ACACB*
288 (Hs00153715_m1), *PPARG* (Hs01115513_m1), *CEBPA* (Hs00269972_s1), *ADIPOQ*
289 (Hs00605917_m1), *FASN* (Hs01005622_m1), *SREBF1* (Hs01088691_m1) and
290 *PLIN1* (Hs00160173_m1) (Life Technologies). Each reaction was normalised to a
291 *beta-2-microglobulin* (*B2M*) control (Hs00984230_m1; Applied Biosystems). For
292 quantifications using SYBR-green, qPCRs were performed using (SsoAdvanced Uni-
293 versal SYBR Green Supermix, BioRad) using the BioRad CFX96 Real-Time PCR
294 Detection System (Biorad). *HDAC9* gene primer sequences were forward:
295 AGTGGCAGAGAGGAGAAGCA and reverse: CAGTTCTCCAGGCTCTGGTC. At
296 least three biological replicates were performed and the data represents the means \pm

297 SEM. A two-tailed t-test was performed using GraphPad Prism (GraphPad software
298 Inc., La Jolla, USA) and p-value < 0.05 was considered to be statistically significant.

299 4.5 Lipid quantification

300 Culture medium was removed and the cells were washed twice with PBS and then
301 fixed with 10 % formalin for 30 min. Fixed cells were washed twice with water and
302 incubated in 60 % isopropanol for 2 min. The alcohol was discarded and the cells
303 were then incubated in an Oil Red O (Sigma) and water solution (3:2) for 5 min. Cells
304 were rinsed four times with water and then 100 % isopropanol was added to extract
305 the red oil. The absorbance was measured at 540 nm on a VERSAmax ELISA mi-
306 croplate reader (Molecular Devices) and analysed using the SoftMax Pro Software
307 (Molecular Devices).

308 4.6 Western blotting

309 Cells were washed twice in ice-cold PBS and harvested in RIPA buffer (Ther-
310 moFisher Scientific) supplemented with protease inhibitors. Cell lysates were centri-
311 fugal at 20,000 x g for 20 min at 4°C and the total protein lysate was quantified using
312 Bradford Reagent (B6916; Sigma). Then, 40 µg of total protein lysate was separated
313 on a 4-12 % Bis-Tris Plus Gel (Life Technologies) and transferred to a nitrocellulose
314 membrane using the iBlot2 Gel Transfer Device (Life Technologies). Membranes
315 were blocked in 0.5 % non-fat dry milk and probed with anti-ABCG1 (1:1000;
316 ab52617, abcam) and antinuclear matrix protein p84 (1:5,000; ab487, abcam) pri-
317 mary antibodies anti-rabbit IgG (1:20,000; Ab205718, abcam) and anti-mouse IgG
318 (1:5,000; A4416, Sigma Aldrich) secondary antibodies for 1 h at room temperature.
319 Membranes were exposed using Clarity Western ECL Substrate (Bio-Rad) and pro-
320 tein bands were detected on a LI-COR Imaging system with C-DiGit Image Studio 4.0
321 software (LI-COR Biosciences, Ltd., UK).

322 4.7 Phosphorylated AKT analysis

323 Differentiated cells cultured in DMEM/F12 medium were serum starved overnight and
324 then washed with PBS and stimulated with or without 200 nM insulin for 1 h in
325 DMEM/F12 (without glucose or serum) at 37°C in 5 % CO₂. The total protein was
326 harvested in RIPA buffer supplemented with protease and phosphatase inhibitors, as
327 described above. The primary antibodies (all used at 1:1,000 dilution unless other-
328 wise stated) used were anti pAKT (S473; Cell Signaling) and anti Akt (9272 - 1:5,000
329 dilution; Cell Signaling) and the secondary antibody used was goat pAb to Rb igG
330 (Ab205718 - 1:20,000 dilution; Abcam). Protein expression studies were also per-
331 formed by WES, an automated capillary-based size separation and nano-
332 immunoassay system (ProteinSimple, San Jose CA, USA - a Bio-Techne Brand),
333 according to manufacturer's protocol, for analysis performed using the Compass for
334 Simple Western software v.4.0. The wes was performed on SGBS samples (1:100)
335 for anti pAKT (S473; Cell Signaling), anti Akt (9272 - 1:100 dilution; Cell Signaling)
336 anti pERK (9102; Cell Signaling) and anti ERK (9101 - 1:100 dilution; Cell Signaling).

337 4.8 Glucose uptake assay

338 A Glucose Uptake-Glo Assay (J1342; Promega) was used to measure glucose up-
339 take in differentiated cells (day 12), according to the manufacturer's protocol. A total
340 of 20,000 cells in 100 µl media were plated in each well of a 96-well white plate. Dif-
341 ferentiated cells were cultured overnight in DMEM/F12 media with no serum. On the
342 day of the assay, the media was replaced with 100 µl DMEM/F12 (without glucose or
343 serum) supplemented with or without 1 µM insulin and incubated for 1 h at 37°C in
344 5 % CO₂. Cells were washed with PBS and 50 µl 1 mM 2-Deoxy-D-glucose (2DG)
345 was added to each well and incubated for 10 min at room temperature. Next, 25 µl
346 Stop Buffer was added followed by 25 µl Neutralization Buffer per well. Finally, 100 µl

347 2DG6P Detection Reagent was added and incubated for 4.5 h at room temperature.

348 The luminescence was recorded on a Mithras LB 940 luminometer (Berthold Tech-

349 nologies) and analysed using the MicroWin Software (Berthold Technologies).

350 4.9 *ABCG1* silencing using shRNA lentiviral vector

351 Undifferentiated SGBS cells were plated at 50 % confluence in 6-well plates and in-

352 fected with commercial lentiviral particles targeting either human *ABCG1*

353 (TRCN0000420907; Sigma) (TAGGAAGATGTAGGCAGATTG) or non-target controls

354 (SHC202) (CCGGCAACAAGATGAAGAGCACCAACTC) and (TRCN0000158395;

355 CCTACAGTGGATGTCCTACAT) (Sigma Aldrich). The transduced cells were se-

356 lected in media containing 1 ug/ml puromycin for 6 days. Stable *ABCG1* KD and con-

357 trol cells were then cultured and differentiated into mature adipocytes, as described

358 above.

359 4.10 Analysis of transcriptomic data from human samples

360 Transcriptomic data (Affymetrix Human Gene 1.1 ST Array) from the GSE71220

361 dataset was downloaded from the GEO database. The subjects analysed were the

362 57 control samples from the Evaluation of COPD Longitudinally to Identify Predictive

363 Surrogate Endpoints (ECLIPSE) study, of which 13 were statin-users (26). In addi-

364 tion, transcriptomic data (Illumina HumanHT-12 WG-DASL V4.0 R2 expression

365 beadchip) from peripheral blood mononuclear cells from the YELLOW II retrospective

366 study (GSE86216) was also downloaded from the GEO dataset. This included blood

367 samples from a total of 85 patients that were analysed before and after an extensive

368 8-12 week statin treatment (27). For both datasets, the data was downloaded and

369 analysed using the R packages GEOquery (45) and limma (48).

370

371 List of abbreviations

372 **B2M:** beta-2-microglobulin

373 **BMI:** body mass index

374 **DMP:** differentially methylated position

375 **DMR:** differentially methylated region

376 **DMSO:** dimethyl sulfoxide

377 **EWAS:** epigenome wide association study

378 **HDAC9:** histone deacetylase 9

379 **KD:** knockdown

380 **SGBS:** Simpson-Golabi-Behmel syndrome

381 **SNP:** single nucleotide polymorphism

382 **T2D:** type 2 diabetes

383

384 Declarations

385 **Ethics approval and consent to participate**

386 Not applicable

387 **Consent for publication**

388 Not applicable

389 **Availability of data and materials**

390 The datasets generated and/or analysed during the current study are available in the

391 Gene Expression Omnibus (GEO) repository, under GSE139211

392 <https://www.ncbi.nlm.nih.gov/geo/query/acc.cgi?acc=GSE139211>. Access to data-

393 sets will remain private during period of manuscript review. Reviewers can access

394 data using the following secure token: yzmzwwkaprgpdj

395 **Competing interests**

396 The authors declare that they have no competing interests.

397 **Funding**

398 This study was supported by non-profit organizations and public bodies for funding of
399 scientific research conducted in France and within the European Union: “*Centre Na-*
400 *tional de la Recherche Scientifique*”, “*Université de Lille 2*”, “*Institut Pasteur de Lille*”,
401 “*Société Francophone du Diabète*”, “*Contrat de Plan Etat-Région*”, “*Agence Nationale*
402 *de la Recherche*”, ANR-10-LABX-46, ANR EQUIPEX Ligan MP: ANR-10-EQPX-07-
403 01, European Research Council GEPIDIAB - 294785.

404 **Authors' contributions**

405 AK, AA, TA, FT and PF designed the project. AK, FT, SM, RB and HC have per-
406 formed the experiments. SL performed the methylome wet lab experiments and MC
407 performed the methylation analysis. AK and MC prepared the figures. AK and PF
408 wrote the manuscript. All authors edited the paper.

409 **Acknowledgements**

410 The authors would like to thank Prof. Dr. M. Wabitsch (University of Ulm, Germany)
411 for kindly providing the SGBS cell line and differentiation protocol.

412

413

414 **References:**

- 415 1. Scherer PE. The Multifaceted Roles of Adipose Tissue—Therapeutic Targets for Diabe-
416 tes and Beyond: The 2015 Banting Lecture. *Diabetes*. 2016 Jun 1;65(6):1452–61.
- 417 2. Arner E, Westermark PO, Spalding KL, Britton T, Rydén M, Frisén J, et al. Adipocyte
418 Turnover: Relevance to Human Adipose Tissue Morphology. *Diabetes*. 2010
419 Jan;59(1):105–9.
- 420 3. Cotillard A, Poitou C, Torcivia A, Bouillot J-L, Dietrich A, Klöting N, et al. Adipocyte
421 size threshold matters: link with risk of type 2 diabetes and improved insulin resistance
422 after gastric bypass. *J Clin Endocrinol Metab*. 2014 Aug;99(8):E1466-1470.
- 423 4. Muir LA, Baker NA, Washabaugh AR, Neeley CK, Flesher CG, DelProposto JB, et al.
424 Adipocyte hypertrophy-hyperplasia balance contributes to weight loss after bariatric sur-
425 gery. *Adipocyte*. 2017 03;6(2):134–40.

- 426 5. Gustafson B, Hedjazifar S, Gogg S, Hammarstedt A, Smith U. Insulin resistance and
427 impaired adipogenesis. *Trends Endocrinol Metab TEM*. 2015 Apr;26(4):193–200.
- 428 6. Lönn M, Mehlige K, Bengtsson C, Lissner L. Adipocyte size predicts incidence of type 2
429 diabetes in women. *FASEB J Off Publ Fed Am Soc Exp Biol*. 2010 Jan;24(1):326–31.
- 430 7. Lönn M, Mehlige K, Bengtsson C, Lissner L. Adipocyte size predicts incidence of type 2
431 diabetes in women. *FASEB J Off Publ Fed Am Soc Exp Biol*. 2010 Jan;24(1):326–31.
- 432 8. Weyer C, Foley JE, Bogardus C, Tataranni PA, Pratley RE. Enlarged subcutaneous ab-
433 dominal adipocyte size, but not obesity itself, predicts type II diabetes independent of in-
434 sulin resistance. *Diabetologia*. 2000 Dec;43(12):1498–506.
- 435 9. Ghaben AL, Scherer PE. Adipogenesis and metabolic health. *Nat Rev Mol Cell Biol*.
436 2019 Apr;20(4):242–58.
- 437 10. Hu E, Liang P, Spiegelman BM. AdipoQ is a novel adipose-specific gene dysregulated
438 in obesity. *J Biol Chem*. 1996 May 3;271(18):10697–703.
- 439 11. Hu E, Tontonoz P, Spiegelman BM. Transdifferentiation of myoblasts by the adipogenic
440 transcription factors PPAR gamma and C/EBP alpha. *Proc Natl Acad Sci U S A*. 1995
441 Oct 10;92(21):9856–60.
- 442 12. Lowe CE, O’Rahilly S, Rochford JJ. Adipogenesis at a glance. *J Cell Sci*. 2011 Aug
443 15;124(16):2681–6.
- 444 13. Braun KVE, Dhana K, de Vries PS, Voortman T, van Meurs JBJ, Uitterlinden AG, et al.
445 Epigenome-wide association study (EWAS) on lipids: the Rotterdam Study. *Clin Epige-
446 netics*. 2017;9:15.
- 447 14. Chambers JC, Loh M, Lehne B, Drong A, Kriebel J, Motta V, et al. Epigenome-wide
448 association of DNA methylation markers in peripheral blood from Indian Asians and Eu-
449 ropeans with incident type 2 diabetes: a nested case-control study. *Lancet Diabetes En-
450 docrinol*. 2015 Jul;3(7):526–34.
- 451 15. Dayeh T, Tuomi T, Almgren P, Perflyev A, Jansson P-A, de Mello VD, et al. DNA
452 methylation of loci within ABCG1 and PHOSPHO1 in blood DNA is associated with fu-
453 ture type 2 diabetes risk. *Epigenetics*. 2016 May 5;11(7):482–8.
- 454 16. Wilson LE, Harlid S, Xu Z, Sandler DP, Taylor JA. An epigenome-wide study of body
455 mass index and DNA methylation in blood using participants from the Sister Study co-
456 hort. *Int J Obes* 2005. 2017 Jan;41(1):194–9.
- 457 17. Nakata M, Nagasaka S, Kusaka I, Matsuoka H, Ishibashi S, Yada T. Effects of statins on
458 the adipocyte maturation and expression of glucose transporter 4 (SLC2A4): implica-
459 tions in glycaemic control. *Diabetologia*. 2006 Aug;49(8):1881–92.
- 460 18. Sattar N, Preiss D, Murray HM, Welsh P, Buckley BM, de Craen AJM, et al. Statins and
461 risk of incident diabetes: a collaborative meta-analysis of randomised statin trials. *Lancet
462 Lond Engl*. 2010 Feb 27;375(9716):735–42.

- 463 19. Wabitsch M, Brenner RE, Melzner I, Braun M, Möller P, Heinze E, et al. Characteriza-
464 tion of a human preadipocyte cell strain with high capacity for adipose differentiation.
465 *Int J Obes Relat Metab Disord J Int Assoc Study Obes.* 2001 Jan;25(1):8–15.
- 466 20. Cao Q, Rong S, Repa JJ, Clair RSt, Parks JS, Mishra N. HDAC9 represses cholesterol
467 efflux and generation of alternatively activated macrophages in atherosclerosis develop-
468 ment. *Arterioscler Thromb Vasc Biol.* 2014 Sep;34(9):1871–9.
- 469 21. Jiang W, Agrawal DK, Boosani CS. Cell-specific histone modifications in atherosclero-
470 sis (Review). *Mol Med Rep.* 2018 Aug 1;18(2):1215–24.
- 471 22. Chambers JC, Loh M, Lehne B, Drong A, Kriebel J, Motta V, et al. Epigenome-wide
472 association of DNA methylation markers in peripheral blood from Indian Asians and Eu-
473 ropeans with incident type 2 diabetes: a nested case-control study. *Lancet Diabetes*
474 *Endocrinol.* 2015 Jul;3(7):526–34.
- 475 23. Demerath EW, Guan W, Grove ML, Aslibekyan S, Mendelson M, Zhou Y-H, et al.
476 Epigenome-wide association study (EWAS) of BMI, BMI change and waist circumfer-
477 ence in African American adults identifies multiple replicated loci. *Hum Mol Genet.*
478 2015 Aug 1;24(15):4464–79.
- 479 24. Rönn T, Volkov P, Gillberg L, Kokosar M, Perfilyev A, Jacobsen AL, et al. Impact of
480 age, BMI and HbA1c levels on the genome-wide DNA methylation and mRNA expres-
481 sion patterns in human adipose tissue and identification of epigenetic biomarkers in
482 blood. *Hum Mol Genet.* 2015 Jul 1;24(13):3792–813.
- 483 25. Frisdal E, Le Lay S, Hooton H, Poupel L, Olivier M, Alili R, et al. Adipocyte ATP-
484 binding cassette G1 promotes triglyceride storage, fat mass growth, and human obesity.
485 *Diabetes.* 2015 Mar;64(3):840–55.
- 486 26. Obeidat M, Fishbane N, Nie Y, Chen V, Hollander Z, Tebbutt SJ, et al. The Effect of
487 Statins on Blood Gene Expression in COPD. *PLOS ONE.* 2015 Oct
488 13;10(10):e0140022.
- 489 27. Chamaria S, Johnson KW, Vengrenyuk Y, Baber U, Shameer K, Divaraniya AA, et al.
490 Intracoronary Imaging, Cholesterol Efflux, and Transcriptomics after Intensive Statin
491 Treatment in Diabetes. *Sci Rep [Internet].* 2017 Aug 1 [cited 2019 Nov 7];7. Available
492 from: <https://www.ncbi.nlm.nih.gov/pmc/articles/PMC5539108/>
- 493 28. Ahmadizar F, Ochoa-Rosales C, Glisic M, Franco OH, Muka T, Stricker BH. Associa-
494 tions of statin use with glycaemic traits and incident type 2 diabetes. *Br J Clin*
495 *Pharmacol.* 2019 May;85(5):993–1002.
- 496 29. Anastasiadi D, Esteve-Codina A, Piferrer F. Consistent inverse correlation between
497 DNA methylation of the first intron and gene expression across tissues and species. *Epi-*
498 *genetics Chromatin [Internet].* 2018 Jun 29 [cited 2019 Oct 9];11. Available from:
499 <https://www.ncbi.nlm.nih.gov/pmc/articles/PMC6025724/>
- 500 30. Yang X, Han H, De Carvalho DD, Lay FD, Jones PA, Liang G. Gene Body Methylation
501 Can Alter Gene Expression and Is a Therapeutic Target in Cancer. *Cancer Cell.* 2014
502 Oct 13;26(4):577–90.

- 503 31. Paton VG, Shackelford JE, Krisans SK. Cloning and Subcellular Localization of Ham-
504 ster and Rat Isopentenyl Diphosphate Dimethylallyl Diphosphate Isomerase A PTS1
505 MOTIF TARGETS THE ENZYME TO PEROXISOMES. *J Biol Chem.* 1997 Jul
506 25;272(30):18945–50.
- 507 32. Wang C-C, Yen J-H, Cheng Y-C, Lin C-Y, Hsieh C-T, Gau R-J, et al. Polygala
508 tenuifolia extract inhibits lipid accumulation in 3T3-L1 adipocytes and high-fat diet-
509 induced obese mouse model and affects hepatic transcriptome and gut microbiota pro-
510 files. *Food Nutr Res [Internet].* 2017 Oct 5 [cited 2019 Oct 14];61(1). Available from:
511 <https://www.ncbi.nlm.nih.gov/pmc/articles/PMC5642193/>
- 512 33. Chatterjee TK, Idelman G, Blanco V, Blomkalns AL, Piegore MG, Weintraub DS, et al.
513 Histone deacetylase 9 is a negative regulator of adipogenic differentiation. *J Biol Chem.*
514 2011 Aug 5;286(31):27836–47.
- 515 34. Chatterjee TK, Basford JE, Yiew KH, Stepp DW, Hui DY, Weintraub NL. Role of his-
516 tone deacetylase 9 in regulating adipogenic differentiation and high fat diet-induced
517 metabolic disease. *Adipocyte.* 2014 Dec 10;3(4):333–8.
- 518 35. Akinyemiju T, Do AN, Patki A, Aslibekyan S, Zhi D, Hidalgo B, et al. Epigenome-wide
519 association study of metabolic syndrome in African-American adults. *Clin Epigenetics.*
520 2018;10:49.
- 521 36. Cardona A, Day FR, Perry JRB, Loh M, Chu AY, Lehne B, et al. Epigenome-Wide As-
522 sociation Study of Incident Type 2 Diabetes in a British Population: EPIC-Norfolk
523 Study. *Diabetes.* 2019 Sep 9;db180290.
- 524 37. Hidalgo B, Irvin MR, Sha J, Zhi D, Aslibekyan S, Absher D, et al. Epigenome-wide as-
525 sociation study of fasting measures of glucose, insulin, and HOMA-IR in the Genetics of
526 Lipid Lowering Drugs and Diet Network study. *Diabetes.* 2014 Feb;63(2):801–7.
- 527 38. Kriebel J, Herder C, Rathmann W, Wahl S, Kunze S, Molnos S, et al. Association be-
528 tween DNA Methylation in Whole Blood and Measures of Glucose Metabolism: KORA
529 F4 Study. *PLoS One.* 2016;11(3):e0152314.
- 530 39. Buchmann J, Meyer C, Neschen S, Augustin R, Schmolz K, Kluge R, et al. Ablation of
531 the Cholesterol Transporter Adenosine Triphosphate-Binding Cassette Transporter G1
532 Reduces Adipose Cell Size and Protects against Diet-Induced Obesity. *Endocrinology.*
533 2007 Apr 1;148(4):1561–73.
- 534 40. Choromanska B, Mysliwiec P, Hady HR, Dadan J, Mysliwiec H, Bonda T, et al. The
535 implication of adipocyte ATP-binding cassette A1 and G1 transporters in metabolic
536 complications of obesity. *J Physiol Pharmacol Off J Pol Physiol Soc.* 2019 Feb;70(1).
- 537 41. Frisdal E, Le Lay S, Hooton H, Poupel L, Olivier M, Alili R, et al. Adipocyte ATP-
538 binding cassette G1 promotes triglyceride storage, fat mass growth, and human obesity.
539 *Diabetes.* 2015 Mar;64(3):840–55.
- 540 42. Mauldin JP, Nagelin MH, Wojcik AJ, Srinivasan S, Skafien MD, Ayers CR, et al. Re-
541 duced expression of ATP-binding cassette transporter G1 increases cholesterol accumu-
542 lation in macrophages of patients with type 2 diabetes mellitus. *Circulation.* 2008 May
543 27;117(21):2785–92.

- 544 43. Tavoosi Z, Moradi-Sardareh H, Saidijam M, Yadegarazari R, Borzuei S, Soltanian A, et
545 al. Cholesterol Transporters ABCA1 and ABCG1 Gene Expression in Peripheral Blood
546 Mononuclear Cells in Patients with Metabolic Syndrome. *Cholesterol*.
547 2015;2015:682904.
- 548 44. Arner P, Bernard S, Appelsved L, Fu K-Y, Andersson DP, Salehpour M, et al. Adipose
549 lipid turnover and long-term changes in body weight. *Nat Med*. 2019 Sep;25(9):1385–9.
- 550 45. Aryee MJ, Jaffe AE, Corrada-Bravo H, Ladd-Acosta C, Feinberg AP, Hansen KD, et al.
551 Minfi: a flexible and comprehensive Bioconductor package for the analysis of Infinium
552 DNA methylation microarrays. *Bioinforma Oxf Engl*. 2014 May 15;30(10):1363–9.
- 553 46. Xu Z, Niu L, Li L, Taylor JA. ENmix: a novel background correction method for
554 Illumina HumanMethylation450 BeadChip. *Nucleic Acids Res*. 2016 Feb 18;44(3):e20.
- 555 47. Leek JT, Johnson WE, Parker HS, Jaffe AE, Storey JD. The sva package for removing
556 batch effects and other unwanted variation in high-throughput experiments. *Bioinforma*
557 *Oxf Engl*. 2012 Mar 15;28(6):882–3.
- 558 48. Ritchie ME, Phipson B, Wu D, Hu Y, Law CW, Shi W, et al. limma powers differential
559 expression analyses for RNA-sequencing and microarray studies. *Nucleic Acids Res*.
560 2015 Apr 20;43(7):e47–e47.
- 561 49. Du P, Zhang X, Huang C-C, Jafari N, Kibbe WA, Hou L, et al. Comparison of Beta-
562 value and M-value methods for quantifying methylation levels by microarray analysis.
563 *BMC Bioinformatics*. 2010 Nov 30;11(1):587.
- 564 50. Peters TJ, Buckley MJ, Statham AL, Pidsley R, Samaras K, V Lord R, et al. De novo
565 identification of differentially methylated regions in the human genome. *Epigenetics*
566 *Chromatin*. 2015 Jan 27;8(1):6.

567

568 Figure Legends

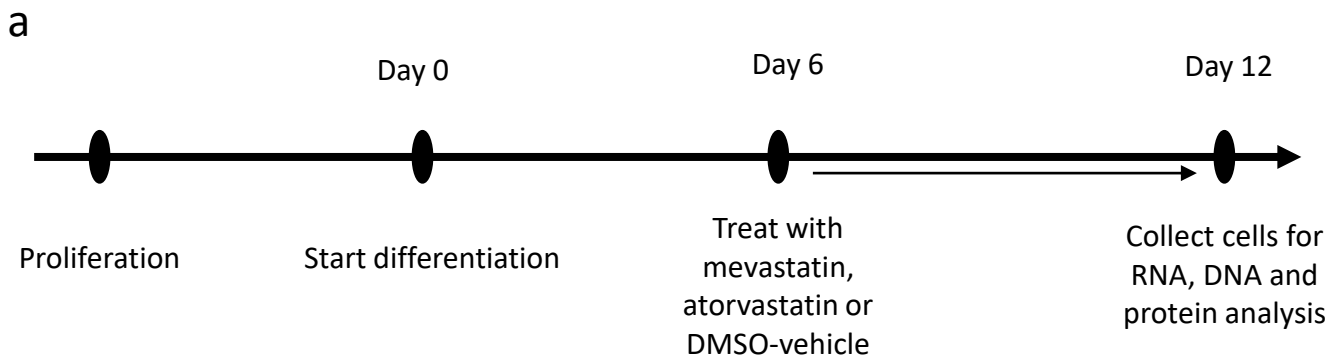
569 **Figure 1: Response of SGBS cell line to statin treatment.** (a) The method used in
570 treating the SGBS cell line at day 6 of differentiation for 6 days. (b) Microscope imag-
571 es showing lipid droplets in statin-treated cells at day 12 of differentiation following
572 statin treatment for atorvastatin, mevastatin and DMSO controls (x10 magnification -
573 scale bar 10 μ m). (c) Expression of key adipose genes for statin-treated cells com-
574 pared to time-matched DMSO controls (normalised to housekeeping gene B2M). * p
575 < 0.05; ** p < 0.01 (d) Protein expression of insulin signalling proteins pAkt and pErk
576 in statin-treated cells compared to controls using WES.

577 **Figure 2: Whole methylome analysis of statin-treated SGBS cells.** (a) Volcano
578 plots of whole methylome results for statin-treated cells (grey indicates log₂ fold
579 change < 1). (b) The hypomethylation of the cg14566882 CpG within the *HDAC9*
580 gene in atorvastatin and mevastatin-treated cells compared to vehicle-treated DMSO
581 cells in the 4 biological replicates (raw β -values shown). (c) The mRNA expression
582 level of *HDAC9* in mevastatin and atorvastatin-treated SGBS cell line. * $p < 0.05$; ** p
583 < 0.01 (d) The protein expression of ABCG1 compared to housekeeping gene p84
584 shows a reduced expression in atorvastatin and mevastatin-treated SGBS cells.

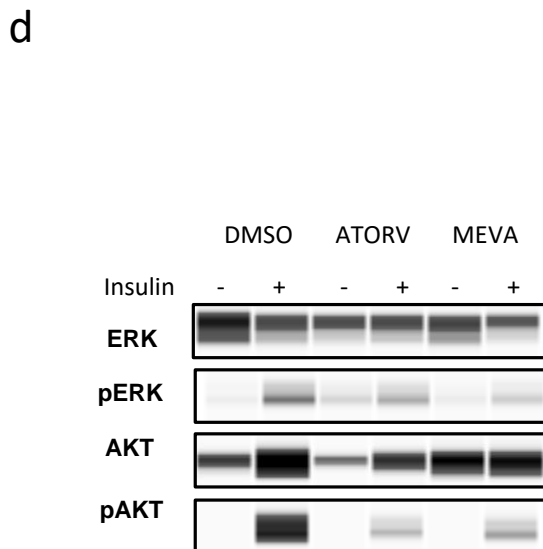
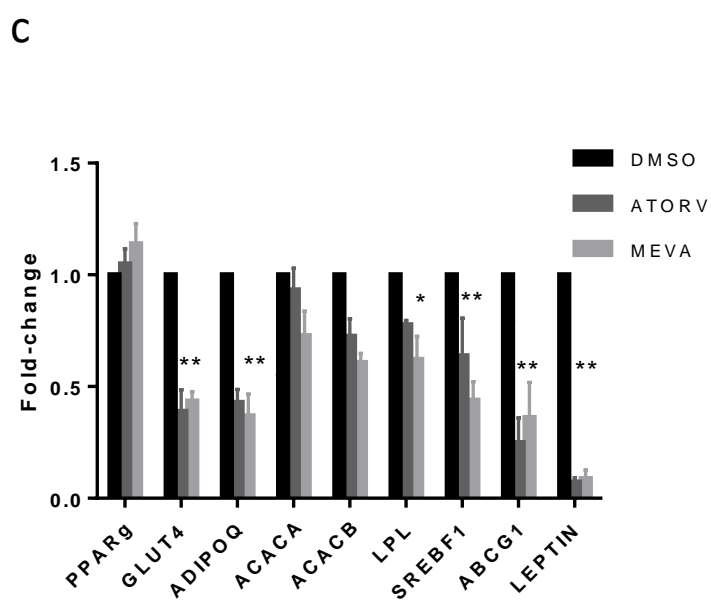
585 **Figure 3: Adipogenesis changes in stably transfected ABCG1 KD cells.** (a)
586 Western Blot protein expression of ABCG1 (a) during differentiation (b) after silencing
587 in SGBS cell lines. (c) Lipid content analysed by red oil of *ABCG1* KD compared to
588 controls. (d) Expression of key adipose genes at day 12 differentiation in KD *ABCG1*
589 cells compared to shRNA controls, normalised to housekeeping gene *B2M* and com-
590 pared to DMSO-vehicle controls. Experiments were performed at $n = 4$ biological rep-
591 licates. (e) Glucose uptake in *ABCG1* KD compared to controls stimulated with or
592 without 1 μ M insulin for 1 hour. Fold change in KD and control cells compared to cells
593 not treated with insulin. (f) Analysis of insulin signalling in SGBS *ABCG1* KD cell line
594 through protein expression of phosphorylated AKT at day 12, stimulated with or with-
595 out 200 nM insulin for 1 hour, using western blot analysis. * $p < 0.05$; ** $p < 0.001$; ***
596 $p < 0.0001$.

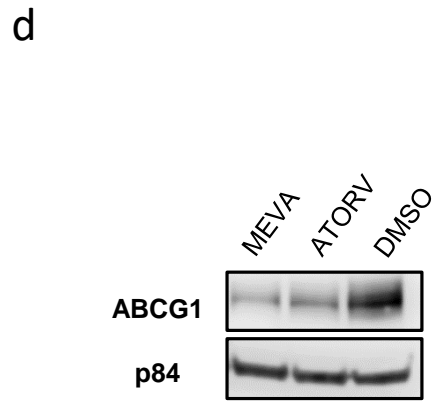
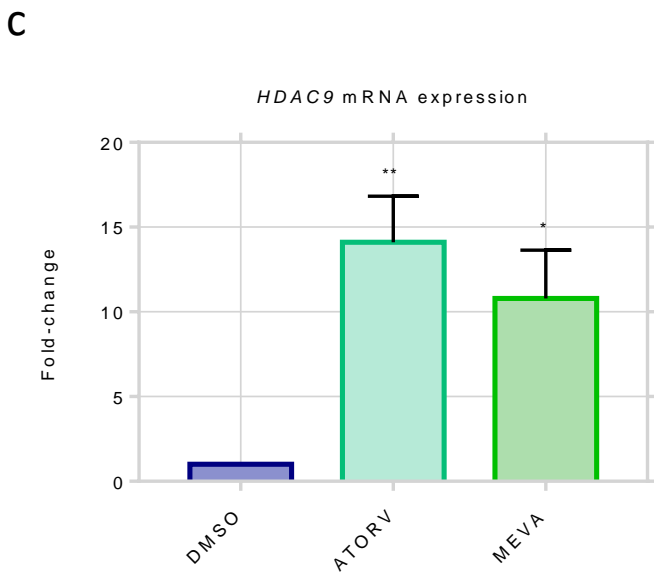
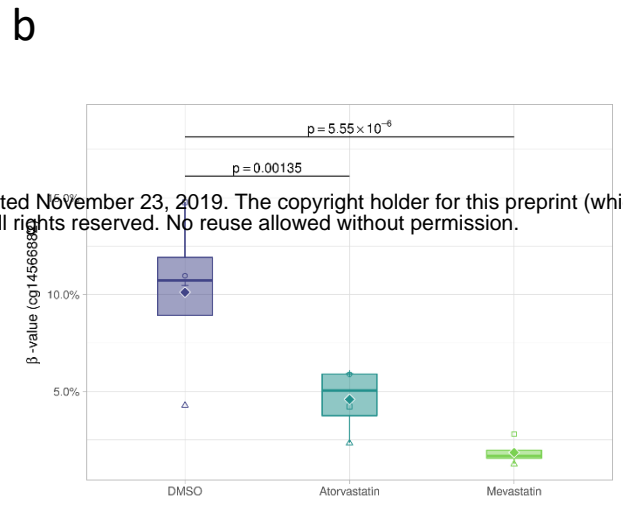
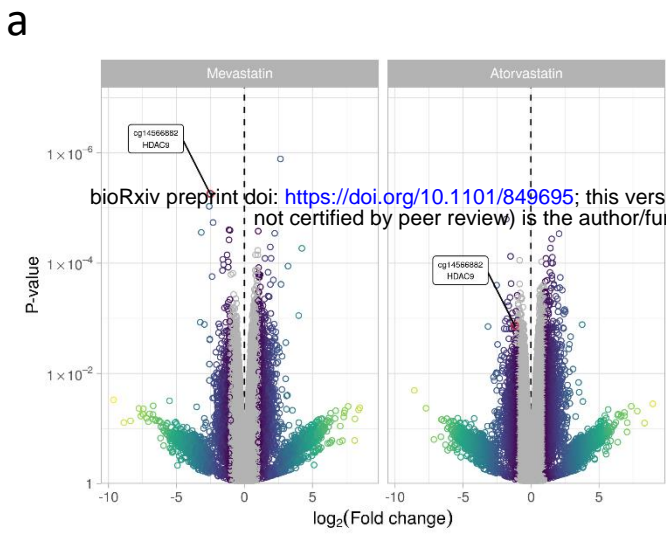
597 **Figure 4: The expression of ABCG1 in human samples.** (a) *ABCG1* expression
598 was reduced in 13 statin-treated individuals compared to control non-users using
599 transcriptomic data. (b) Data from a total of 85 samples, after extensive statin treat-
600 ment for 8-12 weeks, there was a reduction in *ABCG1* expression compared to base-
601 line levels in two probes.

602 **Figure 5: A schematic representation of the role of adipocyte turnover in health**
603 **and disease.** In healthy individuals, preadipocytes differentiate into mature adipo-
604 cytes, which have a role in maintaining insulin sensitivity. However, in response to
605 statins, epigenetic changes in *HDAC9* cause acetylation changes in *ABCG1* and
606 other crucial adipogenesis genes, which in-turn an obstruction of differentiation and
607 metabolic dysfunction.

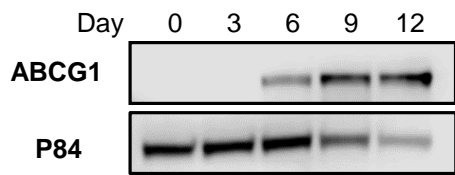


bioRxiv preprint doi: <https://doi.org/10.1101/849695>; this version posted November 23, 2019. The copyright holder for this preprint (which was not certified by peer review) is the author/funder. All rights reserved. No reuse allowed without permission.

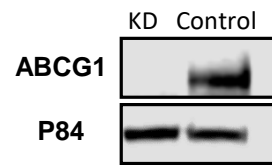




a

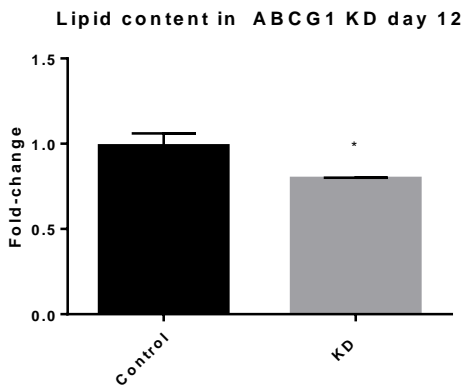


b

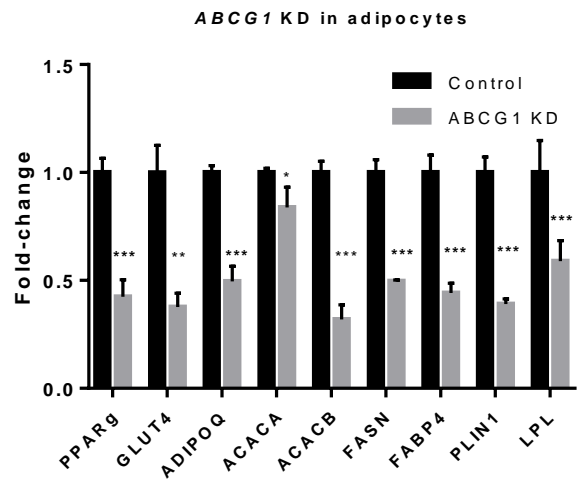


bioRxiv preprint doi: <https://doi.org/10.1101/849695>; this version posted November 23, 2019. The copyright holder for this preprint (which was not certified by peer review) is the author/funder. All rights reserved. No reuse allowed without permission.

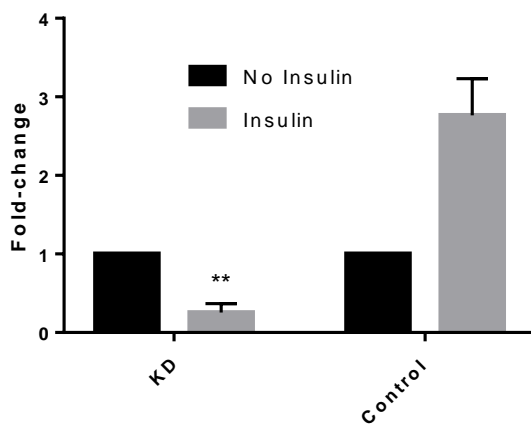
c



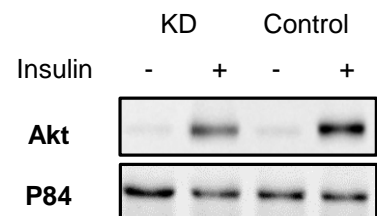
d

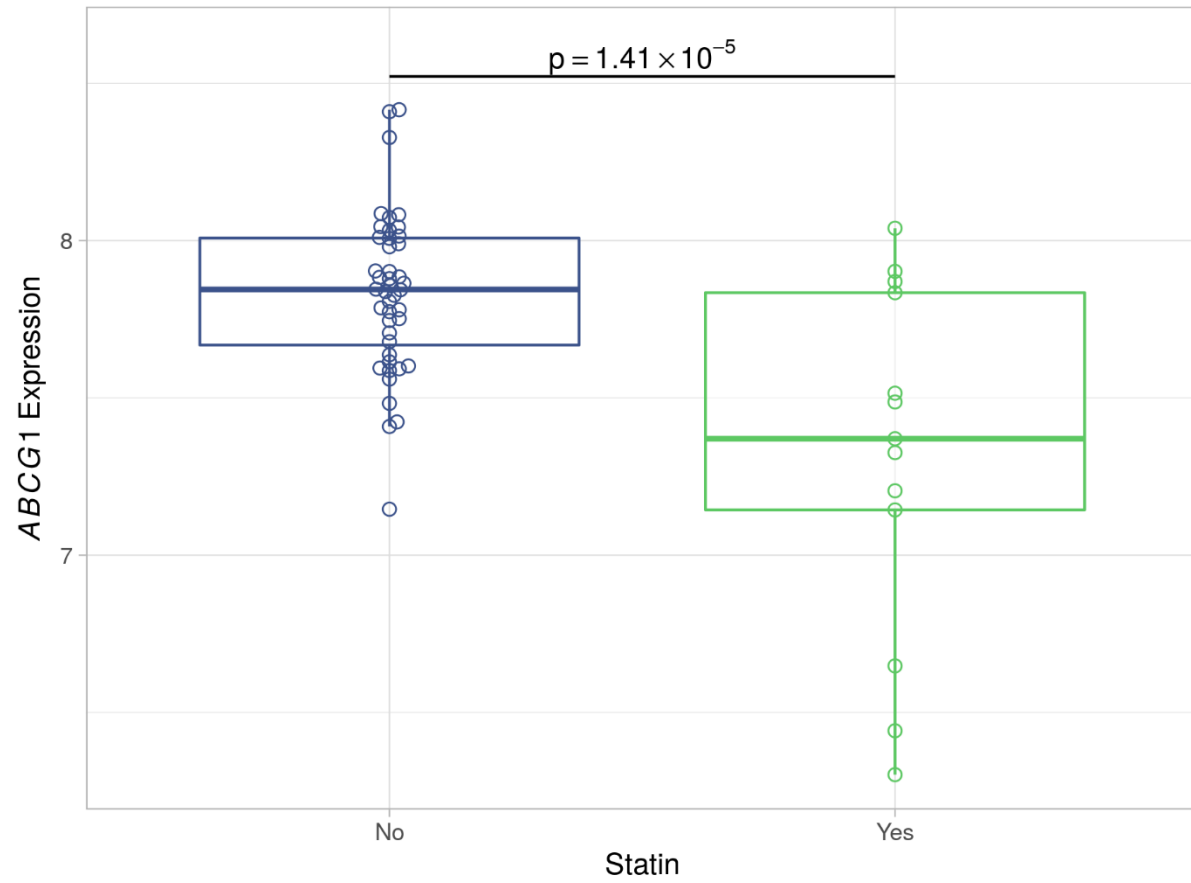
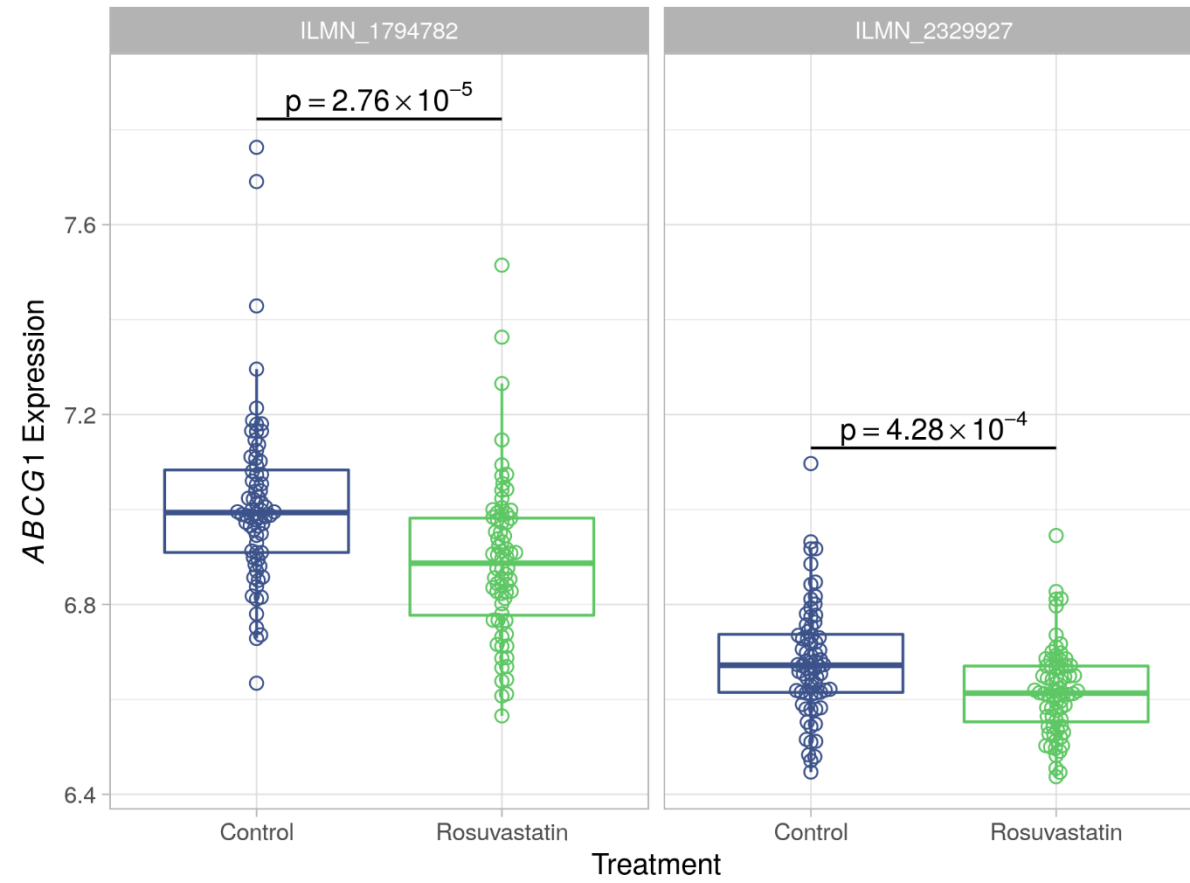


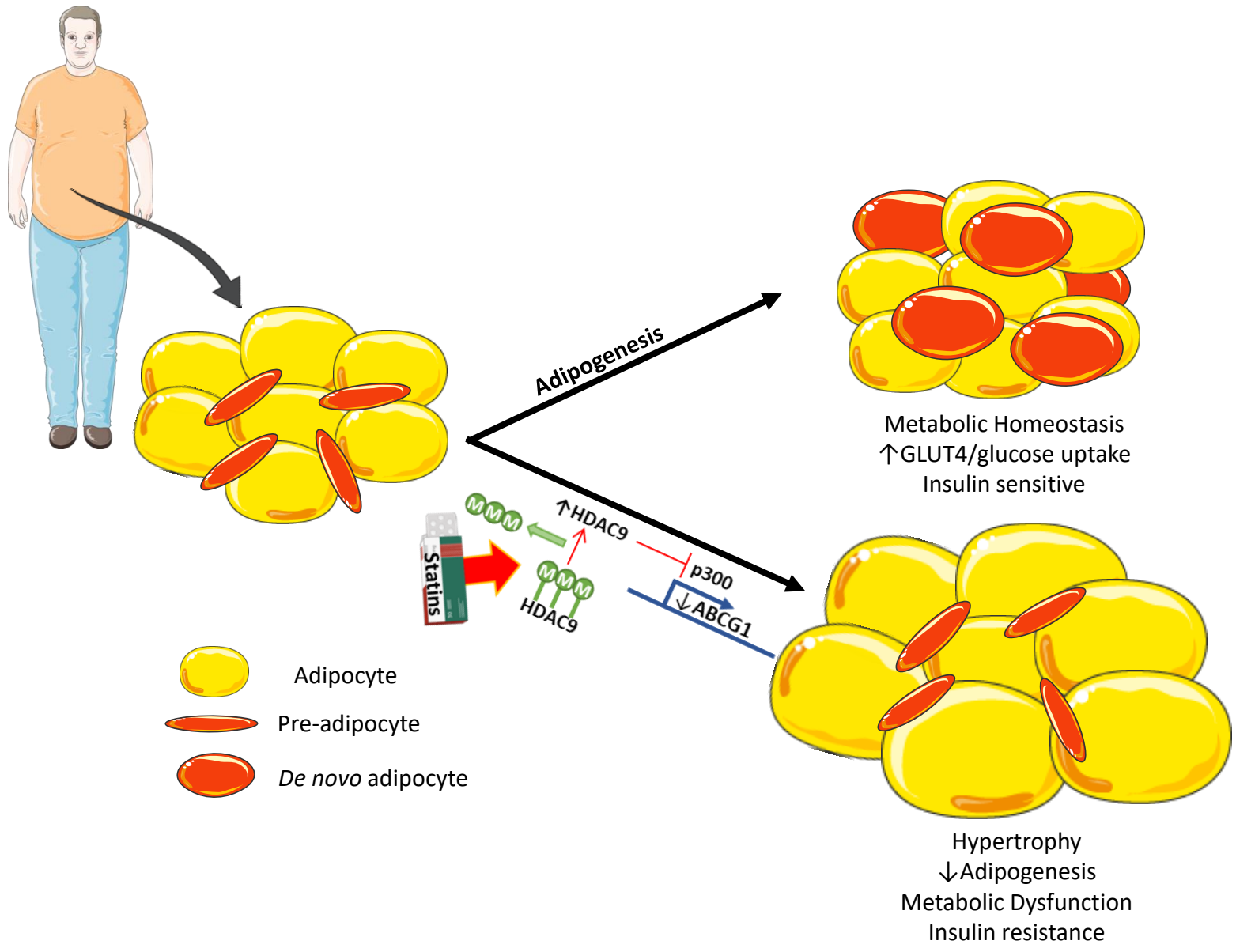
c






d



a**b**



-  Adipocyte
-  Pre-adipocyte
-  *De novo* adipocyte